lubricants

MDPI

Article

Study on Atomization Mechanism of Oil Injection Lubrication for Rolling Bearing Based on Stratified Method

Feng Wei [1,*], Hongbin Liu [1,2] and Yongyan Liu [1]

[1] School of Mechanical and Electrical Engineering, Henan University of Science and Technology, Luoyang 471003, China; hongbin-liu@163.com (H.L.); lyy3396765274@163.com (Y.L.)
[2] Longmen Laboratory, Luoyang 471023, China
* Correspondence: 18237692191@163.com

Abstract: The atomization mechanism of lubrication fluid in rolling bearings under high-speed airflow between the rings was investigated. A simulation model of gas–liquid two-phase flow in angular contact ball bearings was developed, and the jet lubrication process between the bearing rings was simulated using FLUENT computational fluid dynamics software (Ansys 19.2). The complex motion boundary conditions of the rolling elements were addressed through a layered approach. We can obtain more accurate boundary layer flow field changes and statistics of the diameter of oil particles in lubricating oil atomization, which lays the foundation for analyzing the law of influence on lubricating oil atomization. The results show that as the number of boundary layer layers increases, the influence of the boundary layer flow field on the lubricating oil is more obvious. The oil particle size is excessively flat, and the concentration of large particles of oil appears to decrease. As the speed increases, the amount of oil in the cavity decreases, but the oil droplets are also fragmented, which intensifies the atomization and reduces the particle diameter. This reduces the Sauter Mean Diameter (SMD), which is not conducive to the lubrication of the bearing. Under different injection pressures, when the injection pressure is large, it is beneficial to the lubrication of the bearing.

Keywords: angular contact ball bearing; different layers; particle size; different speed; SMD; different injection pressure

Citation: Wei, F.; Liu, H.; Liu, Y. Study on Atomization Mechanism of Oil Injection Lubrication for Rolling Bearing Based on Stratified Method. *Lubricants* **2024**, *12*, 357. https://doi.org/10.3390/lubricants12100357

Received: 15 September 2024
Revised: 12 October 2024
Accepted: 18 October 2024
Published: 18 October 2024

1. Introduction

Under high-speed operating conditions, angular contact ball bearings can support both axial and radial loads. A larger contact angle allows for a greater axial load capacity. Oil injection lubrication is a common method for high-speed rolling bearings, offering a straightforward structure, ease of control, and effective lubrication performance [1,2].

In high-speed operation, lubricating oil in rolling bearings is sprayed through a nozzle to reach the bearing wall. However, some of the oil atomizes due to interactions with the high-speed airflow between the rings and impacts from the airflow. Under centrifugal force, these atomized oil droplets are unable to effectively enter the lubrication zone, which negatively impacts the lubrication and cooling performance of the bearing. The lubricating oil entering between the bearing rings interact with the high-speed air flow between the bearing rings to form a gas–liquid two-phase flow [1,3]. The two-phase flow formed between the bearing rings by oil injection is fundamentally different from the two-phase flow formed by oil–gas and oil–mist lubrication [4–8]. This two-phase flow condition has a certain effect on bearing heat transfer and lubrication. Oil injection lubrication is usually used for bearings running at higher speeds under low or medium load. It is mainly a method of high-pressure injection to inject lubricating oil into the bearing to lubricate it. Therefore, this article uses oil injection lubrication to make the oil enter the bearing cavity to study the atomization of the oil in the process of entering the cavity.

In recent years, some scholars have studied bearing atomization under different parameter conditions. For example, Glahn [9–12] et al. used phase Doppler particle

analyzer (PDPA) technology and numerical calculation methods to study the motion analysis of oil particles in aero-engine bearing cavity, which laid a foundation for the research on particle motion track tracking in the future. Szydlo et al. [13] studied that the change in oil/air ratio has an important influence on the change of oil mist in the pipeline. Lee [14] et al. changed the number of nozzle holes without changing the total orifice outlet area, and used two-dimensional PDPA (phase Doppler particle analyzer) to measure the SMD (Sauter Mean Diameter) and AMD (arithmetic average diameter) droplet diameters. Di et al. [15] designed a fan nozzle system and conducted atomization experiments to analyze the effects of oil pressure difference, sector angle, and outlet height on flow and atomization characteristics. Additionally, the influence of temperature, velocity, and fuel supply variations on the mean diameter of the droplets was examined. Chen [16] et al. used a phase Doppler particle analyzer (PDPA) and high-speed photography to measure the particle characteristics of the spray field of V-shaped cross-hole high-perturbation nozzles and single-hole nozzles with different included angles and different pore size structures. At present, research on bearing atomization at home and abroad mainly focuses on the bearing oil film pressure distribution and its influence on bearing performance at high speed or ultra-high speed.

At higher speeds, the oil atomizes after entering the bearing cavity. Due to the opening of the groove, the oil can enter the bearing through the nozzle to achieve better lubrication. However, after the oil enters the bearing cavity, the influence of high-speed airflow and other factors on the oil in the lower cavity causes the phenomenon of atomization. The reduction of oil particle size does not decrease friction loss or surface wear during bearing operation, nor does it enhance cooling effectiveness. Building on previous studies [17,18], this paper examines the layered processing of rolling elements under complex moving boundary conditions. The research focuses on how oil atomizes into very small droplets due to turbulent radial velocity distribution and the relative movement of surrounding air after entering the bearing cavity from the nozzle and being influenced by the groove. Additionally, it analyzes the variation in oil particle diameter under different layering, rotational speeds, and injection pressures, as well as the trend of the mean diameter of droplets (SMD) over time and at varying speeds. By observing changes in oil particle size, this study aims to provide deeper insights into the atomization characteristics of oil within the cavity.

2. Numerical Calculation Model

2.1. Governing Equations

2.1.1. $k-\varepsilon$ Model

Because high-speed angular contact ball bearings are in a gas–liquid two-phase flow state, the flow system in the cavity is considered to be two incompressible and incompatible fluids, but each phase still meets the basic governing equations of fluid mechanics (the first phase is air, and the second phase is oil).

Without considering the change in the temperature field, assuming that the gas-phase medium is adiabatic and incompressible viscous air, the continuity equation of the gas-phase medium flow between the bearing rings is:

$$\frac{\partial}{\partial x_i}(u_i) = 0 \tag{1}$$

u_i—velocity vector.

Momentum equation

$$\frac{\partial(u_i)}{\partial t} + \frac{\partial(u_i u_j)}{\partial x_i} = -\frac{1}{\rho}\frac{\partial p}{\partial x_i} + \frac{\partial}{\rho \partial x_j}\left(\mu \frac{\partial u_i}{\partial x_i}\right) + S_i \tag{2}$$

In the formula u_j is the velocity vector in the j direction; ρ represents the density, μ represents the dynamic viscosity of the gas-phase medium; p represents the gas-phase

medium pressure; and S_i represents the generalized source term, where the values of i and j are 1, 2, and 3.

The equations of the $k-\varepsilon$ model can make the whole equation closed, which is convenient for solving the turbulence problem. Due to the high-speed operation of the bearing, the gas–liquid two-phase shear flow in the bearing cavity will be violent, and eddy currents will be easily generated under the action of fluid viscosity and the wall surface. In order to make the numerical simulation closer to the actual situation, the turbulence model in this paper, the $k-\varepsilon$ turbulence model [19], is selected for simulation calculation. Then Equation k and Equation ε are as follows:

$$\frac{\partial}{\partial t}(\rho k)+\frac{\partial}{x_i}(\rho k u_i)=\frac{\partial}{x_j}\left[\left(\mu+\frac{\mu_{\mathrm{t}}}{\sigma_{\mathrm{k}}}\right)\frac{\partial k}{\partial x_j}\right]+G_{\mathrm{k}}-\rho\varepsilon-Y_{\mathrm{m}}+G_{\mathrm{b}}+S_{\mathrm{k}} \tag{3}$$

$$\frac{\partial}{\partial t}(\rho\varepsilon)+\frac{\partial}{x_i}(\rho\varepsilon u_i)=\frac{\partial}{x_j}\left[\left(\mu+\frac{\mu_t}{\sigma_\varepsilon}\right)\frac{\partial\varepsilon}{\partial x_j}\right]+G_{1\varepsilon}\frac{\varepsilon}{k}(G_k+C_{3\varepsilon}G_b)-G_{2\varepsilon}\rho\frac{\varepsilon^2}{k}+S_\varepsilon \tag{4}$$

where k is turbulent kinetic energy; ε denotes the rate of turbulent kinetic energy dissipation. The variable ρ signifies density, G_k is the production term of turbulent kinetic energy k due to the mean velocity gradient, while G_b is the generation term caused by buoyancy. Y_m represents the contribution of pulsation expansion in compressible turbulence. The model constants are $C_{1\varepsilon}$ = 1.42, $C_{2\varepsilon}$ = 1.68; $C_{3\varepsilon}$ represents empirical constants; σ_k and σ_ε are the reciprocal of the turbulent Prandtl numbers (Pr) for the turbulent kinetic energy k the dissipation rate. S_k and S_ε represent the custom source terms. Indices i and j can take values 1, 2, or 3, and the empirical constants in the formula are applicable under certain circumstances.

2.1.2. Calculation Model

This paper discusses the grid layering of rolling elements in bearings under complex boundary conditions, inspired by the domain decomposition method. The establishment of the three-dimensional model can more accurately explore the changing law of oil particle size distribution in the bearing cavity and the distribution of oil atomization. The domain decomposition method is a numerical calculation method that decomposes the computational domain into several subdomains, solves them separately, and calculates them comprehensively. This method is easily applicable to mathematical models and calculation formats tailored to each subdomain's characteristics, enhancing overall practicality and facilitating the use of parallel algorithms to accelerate calculations.

In simple terms, the region decomposition algorithm divides the domain into several normalized subregions, transforming the solution of the original problem into solutions for each subregion.

Under the guidance of the domain decomposition method, the rolling elements are divided into different layers (6 layers, 8 layers, and 10 layers). The rolling elements can be categorized into varying layers. However, an increase in the number of layers results in a slower calculation rate of the bearing model, thereby reducing efficiency. Conversely, fewer layers may insufficiently capture the oil atomization dynamics within the cavity. Therefore, this article discusses the change of the oil in the cavity when the rolling elements are divided into 6 and 10 layers. Figure 1 is a simplified model of the bearing. The nozzle position is determined by the results of previous research [20]. In order to make the oil better enter the bearing cavity and satisfy the lubrication of the bearing, an arc-shaped groove is established on the inner wall of the outer ring of the bearing. The groove direction is 60°, the length is 3.5 mm, and the width is 0.65 mm. Figure 1 illustrates the case when the rolling element is divided into 10 layers, and then the model is meshed by software. Because the bearing model is irregular and it is not easy to divide the mesh, the unstructured tetrahedral mesh is used to divide the nozzle and the rolling element. The bearing clearance is locally refined, as shown in Figure 2, and Table 1 is a comparative analysis of different layered values.

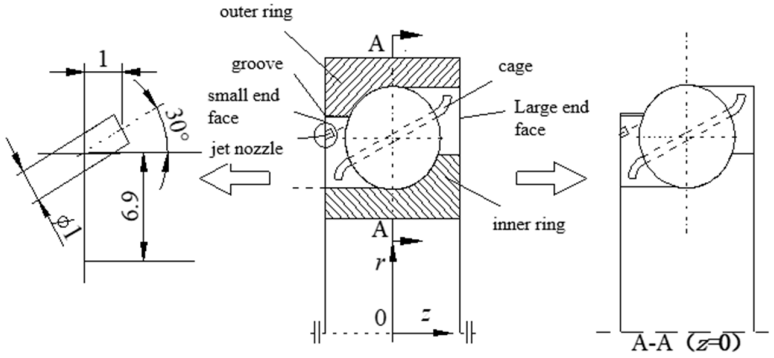

Figure 1. Simplified bearing model and nozzle position. (Unit: mm).

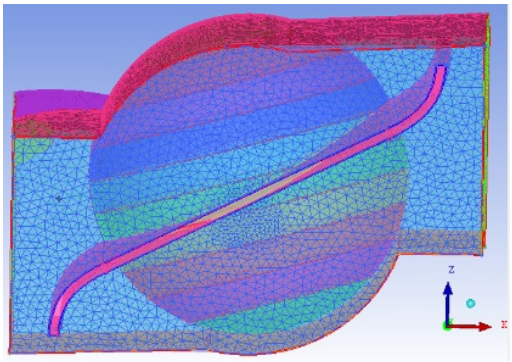

Figure 2. Mesh generation the bearing model (10 layers).

Table 1. Comparative analysis of different stratification values.

Number of Layers	Number of Grids	Number of Iterations	Convergence Accuracy	Calculation Time/Thousand Steps (h)
6	501,345	614	10^{-4}	12.8
8	514,876	581	10^{-4}	13.4
10	548,064	563	10^{-4}	15

2.1.3. The Uniformity of Oil Atomization

The oil is induced into the bearing cavity through the nozzle and the groove. Under the influence of high speed and air within the cavity, the oil droplets become atomized. However, the atomization of the oil droplets is not uniform; thus, relying solely on the average diameter of the oil droplets is insufficient to fully represent the degree of atomization. A more comprehensive approach would involve expressing both the size of the droplet particle diameters and the number and quality of droplets across different diameters. Unfortunately, a complete expression for this is still lacking. The Rosin–Rammler relationship has been utilized thus far:

$$R = 100 \exp\left[-\left(\frac{D_i}{\overline{D}}\right)^n\right]\% \quad (5)$$

In the formula, D_i represents the droplet diameter; n is an index of the uniformity of droplet distribution, usually $1.8 \leq n \leq 4$; R represents the percentage of the total mass of droplets that exceed a diameter of D_i relative to the mass of all droplets; $\overline{D}$ is the size constant; i takes 1, 2, or 3.

When oil enters the bearing cavity through the nozzle, the resulting atomization field exhibits an uneven distribution, characterized by a significant difference between the maximum and minimum droplet diameters. Therefore, the average droplet diameter serves as the indicator of atomization fineness. Typically, a relatively uniform atomization field

is employed to represent the actual atomization field with varying oil droplet sizes. The particle diameter of this uniform atomization field is the average diameter of the droplets in the actual atomization field. The expression has volume average diameter and Sauter Mean Diameter (SMD). Since the size of the droplet diameter is not uniform, assuming that the liquid is sprayed from a high-speed nozzle and atomized into a large number of small droplets, the smallest droplet diameter is 0; then:

The average surface area diameter is expressed as:

$$D_{20} = \left(\frac{\int_{D_{\min}}^{D_{\max}} D^2 \mathrm{d}N}{\int_{D_{\min}}^{D_{\max}} \mathrm{d}N} \right)^{1/2} \tag{6}$$

The volume average diameter is expressed as:

$$D_{30} = \left(\frac{\int_{D_{\min}}^{D_{\max}} D^3 \mathrm{d}N}{\int_{D_{\min}}^{D_{\max}} \mathrm{d}N} \right)^{1/3} \tag{7}$$

Sauter Mean Diameter is expressed as:

$$D_{32} = \frac{\int_{D_{\min}}^{D_{\max}} D^3 \mathrm{d}N}{\int_{D_{\min}}^{D_{\max}} D^2 \mathrm{d}N} \tag{8}$$

where N is the number of droplets with a diameter of D.

3. Geometry Model and Meshing

3.1. Geometric Model

The model of angular contact ball bearing in this article is 7306 as the research object, and its structural parameters are shown in Table 2. The space between the bearing rings is the calculation domain of the model. Due to the lengthy computation time required for the overall model, the analysis simplifies the model by retaining only the inner and outer ring walls while omitting the rolling elements and cage. A 1/12 bearing model is then employed for numerical simulation and analysis.

Table 2. Bearing parameters.

Outer Diameter/mm	Inner Diameter/mm	Bearing Width/mm	Contact Angle/(°)	Number of Steel Balls/mm
72	30	19	15	12

The overall model is divided using unstructured grids. The number of grids is 2,867,328. The number of grids in the overall model is too large. Due to the periodic characteristics of the rolling bearing motion, the calculation time is long for the entire rolling bearing and it is difficult to complete the numerical simulation analysis. "The calculation object is taken as 1/12 of the integral bearing model, including a rolling body". A groove is established to induce oil into the bearing cavity for lubrication; therefore, a single-period grid model with grooved nozzles is used. In this paper, ICEM CFD (Integrated Computer Engineering and Manufacturing Computational Fluid Dynamics) methods are used to conduct gas-phase numerical simulation analysis of rolling bearings.

3.2. Boundary Setting and Numerical Analysis Method

Due to the previous research on the bearing by gas flow, the nozzle is set as the velocity inlet, the small end face is the pressure inlet, and the large end face is the pressure outlet. The nozzle is fixed, and the bearing inner ring, cage, and rolling elements impose

corresponding rotational boundary conditions. The rotational speeds of the rolling elements and the cage can be calculated as:

$$n_{\mathrm{m}} = \frac{n_i}{2}(1 - \frac{D_{\mathrm{w}} \cos \alpha}{d_{\mathrm{m}}}) \tag{9}$$

Here, n_i is the inner ring speed, α is the contact angle, D_{w} is the rolling element pitch circle diameter, and d_{m} is the bearing pitch circle diameter. At the same time, this article also considers the rotational speeds of the rolling elements, which are achieved by setting different speed boundaries on the outer surface of the rolling elements. Due to the layering of the rolling elements in this article, different speed boundaries are established for the rolling elements. Additionally, through stratification, accurate calculation and analysis of the boundary layer oil size at different rotation speed positions of rolling elements can be carried out.

The VOF (Volume of Fluid) model is a surface tracking method, that is, when you need to obtain one or more interfaces that do not bind to fluids under a fixed Euler grid, you can use this model. This paper uses the VOF multiphase flow model to capture the distribution and movement of the gas–liquid two-phase flow inside the bearing cavity and uses the discrete phase model to obtain the distribution of oil particle sizes. The specific calculation parameters are presented in Table 3 below.

Table 3. Specific calculation parameters.

Parameter	Main Phase (Air)	Secondary Phase (60CST Turbine Oil)
Density/(kg/m^3)	1.225	876
Viscosity/(Pa·s)	1.79×10^{-5}	0.05877

The speed is specified based on the design conditions of high-speed rolling bearings. The standard wall function method is applied at the wall surface, while the other boundaries are defined as adiabatic solid walls with a non-slip condition.

When the oil enters the bearing cavity, it is driven by external force; the liquid enters from the nozzle and the groove is induced to enter the bearing cavity. The turbulent radial velocity and the interaction with the surrounding air cause the liquid to be atomized into small droplets. The discrete phase model (DPM) is also known as the particle trajectory model. For the multiphase flow formed by a continuous medium and a discontinuous medium, the continuous fluid is called the continuous phase, and the discontinuous material is called the dispersed phase. We define the discrete phase by setting the boundary conditions of the discrete phase model in the model setting panel, and solve it through calculations. In the result post-processing, we select particle tracking, particle diameter, etc. to analyze the oil particle size in the discrete phase.

4. Results and Analysis

4.1. The Effect of Rolling Element Layering on the Particle Size Between Bearing Rings

When the rolling elements of the bearing are in different layers, the oil entering the groove through the nozzle remains consistent. After stratification, the distribution characteristics of oil at different locations can be accurately analyzed. Figure 3 shows the distribution diagram of the oil particle size of the cross section at z = 0 in the axial direction. In Figure 3a,b, the rolling elements are layered. After the oil enters the bearing cavity, the varying layers of rolling elements generate distinct vortices that influence the distribution of oil within the cavity. Consequently, the atomization distribution of the oil also varies throughout the cavity. When the rolling element is divided into six layers, the size of the vortex formed is not nearly the same because of the different boundary conditions set by the layering. Therefore, the oil with large particle size is mostly distributed between the small end face and the cage, while the oil with large particle size is less noticeable in the area near the rolling body. When the rolling body is divided into 10 layers, the oil in the

cavity is influenced by eddy currents, so that the oil with large particle size will spread and the oil with small particle size will increase. The atomization distribution becomes more pronounced. Thus, when the rolling elements are more stratified, the oil atomization distribution in the cavity is more obvious.

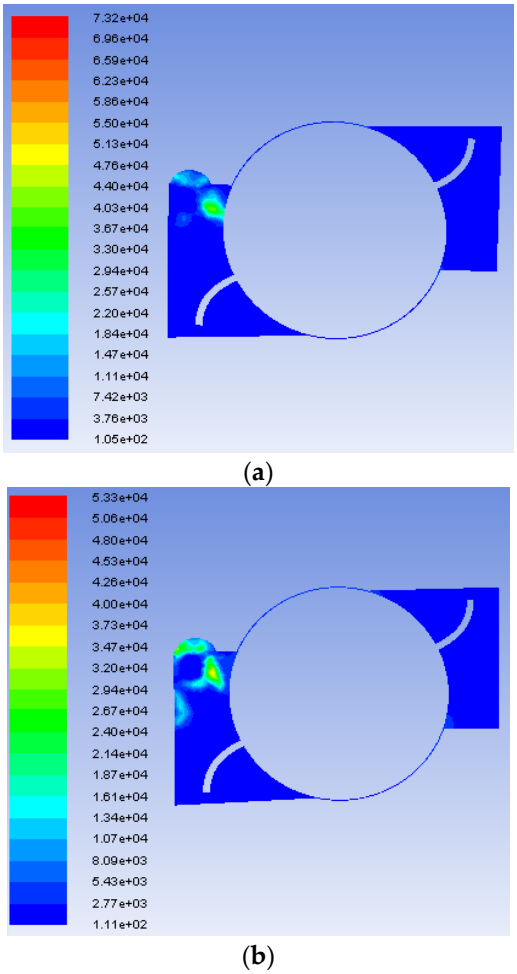

Figure 3. Oil phase cloud image of oil particle size distribution in the cavity with different layers of rolling body. (**a**) Turbulence intensity distribution diagram of rolling body in 6 layers at axial section (z = 0), (**b**) Turbulence intensity distribution diagram of rolling body in 10 layers at axial section (z = 0).

It can be seen from Figure 4 that when the rolling elements are divided into six layers in Figure 4a, the oil in the bearing cavity is affected by its stratification, and the particle size distribution of the oil in the cavity changes significantly. The large particle size oil diffuses, and the oil near the small end face decreases. Although it is affected by the airflow, the large-size oil is still distributed near the rolling elements. As shown in Figure 4b, dividing the rolling element into 10 layers still results in influence from the vortex generated by the airflow. However, the large-diameter oil gradually diffuses between the outer ring raceway and the rolling elements. Increased stratification significantly alters turbulence intensity, enhancing oil diffusion within the bearing cavity. However, during this diffusion process, larger oil droplets experience minimal change, indicating that the varying stratification of the rolling elements affects the distribution of oil atomization in the bearing cavity.

From the comparison of the results of Figures 3 and 4, after the oil enters the bearing cavity, when the rolling elements are in different layers, the oil distribution in the cavity is not the same. Dividing the rolling elements into 10 layers enhances oil distribution dispersion, facilitating clearer visualization of oil atomization in the bearing cavity—an effect not observed in prior bearing studies.

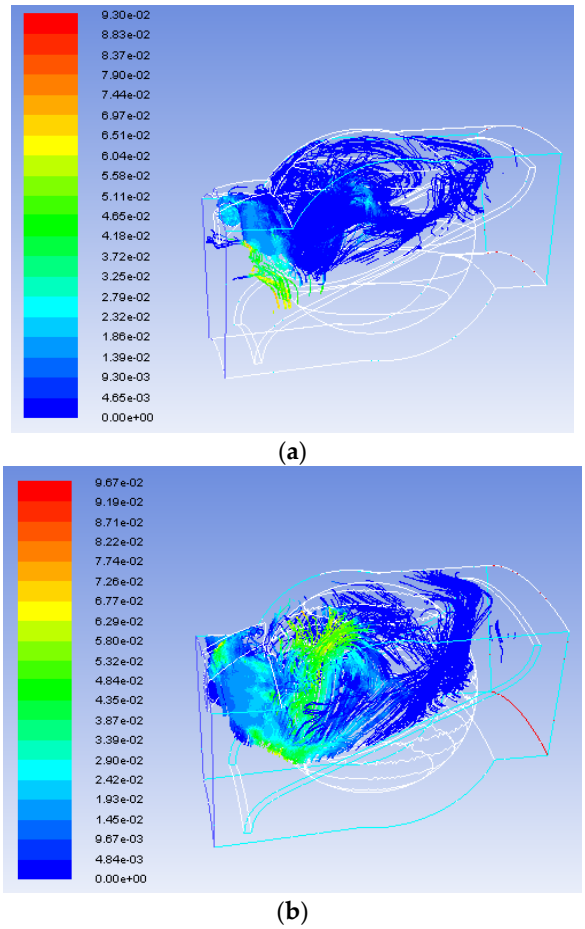

Figure 4. Cloud diagram of the change of oil particle size in different layered cavities of rolling elements at the same time. (**a**) The rolling body is divided into 6 layers, (**b**) The rolling body is divided into 10 layers.

4.2. Oil Atomization in Different Layered Bearing Cavities of Rolling Elements at the Same Time

Figure 5 depicts the change in the percentage of oil particle size in the cavity under the condition of different layers of rolling elements at the same time when the speed is 1.0×10^5 r/min. The atomization of oil between bearing rings can be seen from the change in the percentage of particle size. As illustrated in the figure, when the rolling body is divided into 10 layers, the oil particle size increases up to 40 μm. However, beyond this size, airflow resistance within the bearing cavity and cage causes larger oil droplets to break apart, significantly reducing the proportion of larger oil particles. When the rolling body is divided into 10 layers, the oil with larger particle size is relatively larger. However, with the increase in time, the oil of large particle size decreases less, and the atomization is less, which is still conducive to the lubrication of the bearing. When the rolling body is divided into six layers, the proportion of large oil particles is relatively low. The greater influence of eddy currents in the cavity exacerbates atomization and further reduces the presence of larger oil droplets, which is detrimental to bearing lubrication.

Further analysis of Figure 5 reveals the relationship between oil droplet size percentage and the degree of atomization as follows:

1. Oil droplet size significantly impacts atomization: smaller droplets are more easily carried away by airflow, enhancing atomization, while larger droplets tend to aggregate into a liquid film, leading to decreased atomization. Thus, an increase in droplet size generally results in reduced atomization.
2. The configuration of rolling elements affects fluid flow characteristics. A greater number of layers can create complex flow patterns, such as vortices, that influence

oil droplet dispersion and atomization. Specifically, increased layers may facilitate droplet collisions and merging, resulting in fewer smaller droplets and reduced atomization. Additionally, air resistance is significant, as larger droplets are more prone to breakup, which can enhance atomization. Therefore, the relationship between oil droplet size and atomization is non-linear and impacted by factors such as fluid dynamics, air resistance, and lubrication effectiveness.

3. Atomization degree significantly impacts lubrication performance: moderate atomization enhances coverage, while excessive atomization can rupture the oil film, compromising efficiency.
4. Maintaining an optimal balance of oil droplet size and atomization is crucial for effective lubrication performance.

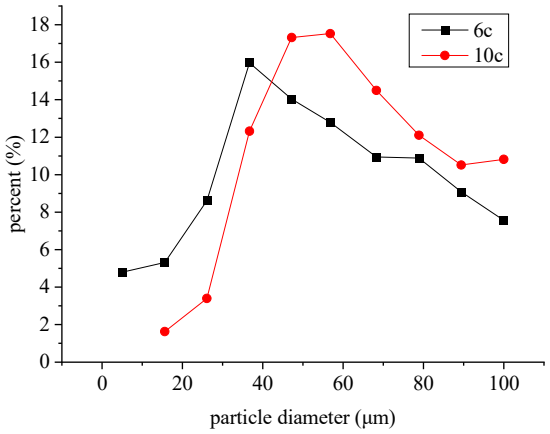

Figure 5. Variation of oil particle size of different layers of rolling elements at the same time.

4.3. The Influence of Different Speeds on the Characteristics of Oil Atomization in the Cavity

Figure 6 presents a distribution diagram of the SMD of the mist field oil in the case of different rotation speeds and different stratifications with time changes of the rolling elements in the cavity. As shown in the figure, when the rolling body is in different layers, the oil particle size at the surface is initially small, and the volume of oil entering the bearing cavity through the groove is limited. Consequently, the proportion of large oil particles is also low, resulting in a reduced amount of oil reaching the rolling body and a small Sauter Mean Diameter (SMD) of the oil particles at the outset. With the change of time, the oil in the bearing cavity gradually increases, the SMD of the oil particles is higher, the atomization quality is poor, and the lubrication effect is better. As time increases and rotation speed rises, strong airflow and the rolling body contribute to a decrease in the size of large oil particles, leading to enhanced atomization. Consequently, the Sauter Mean Diameter (SMD) gradually decreases, improving atomization quality but adversely affecting bearing lubrication. However, when the rolling elements are divided into 10 layers, the more stratified arrangement results in a smaller vortex around them, leading to a reduced influence on the oil in the cavity. Therefore, when the rolling elements are divided into 10 layers, the impact on bearing lubrication is relatively small, which is beneficial to the lubrication of the bearing.

Figure 7 shows the change curve of oil particle size at the same time with different speeds and layers. The variation in oil particle size reflects the atomization process within the cavity. As shown in the figure, different rotational speeds influence oil particle size changes. For rolling elements divided into six layers, at a speed of 1.0×10^5 r/min, the particle size trend increases until it reaches 35 μm. At 1.5×10^5 r/min, this trend continues up to 40 μm. Beyond this point, as further increases in speed occur, air resistance affects larger oil particles, causing their size to gradually decrease. Due to the high speed, larger particles are more significantly impacted, leading to a faster reduction in their proportion, while smaller particles increase, potentially resulting in atomization.

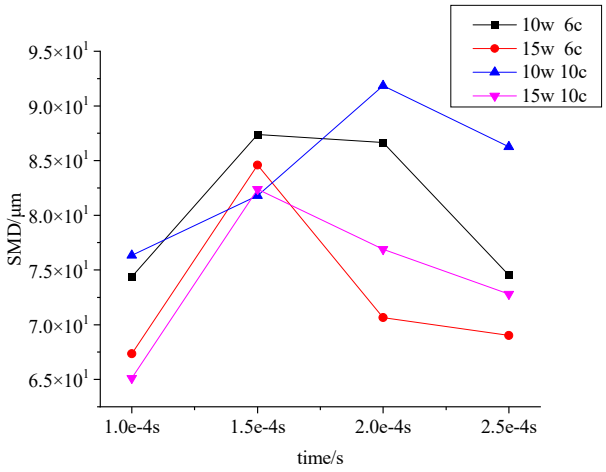

Figure 6. SMD change curve at different speeds and different layers.

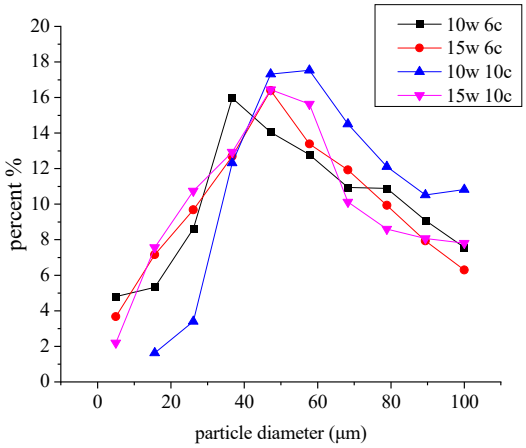

Figure 7. Variation of particle size of different layers of oil at different speeds.

In contrast, when the rolling elements are divided into 10 layers, the upward trend in particle size persists up to 45 μm at 1.0×10^5 r/min. Here, larger particles are more prevalent due to reduced turbulence intensity near the rolling elements, which benefits lubrication as a significant volume of oil enters the bearing cavity. However, at 1.5×10^5 r/min, the high speed limits oil entry into the bearing cavity. Additionally, the cage effect reduces the presence of larger particles, which may lead to atomization. Thus, at elevated rotational speeds, regardless of layer stratification, larger oil particles in the bearing cavity diminish while smaller particles increase, exacerbating atomization and compromising lubrication effectiveness.

4.4. Oil Atomization in the Cavity Under Different Layers and Different Injection Pressures

Figure 8 shows the change of the oil particle size in the bearing cavity under different injection pressure conditions when the rolling elements are divided into six layers at a constant speed of 1.0×10^5 r/min. From the figure, it can be seen that when the injection pressure is 0.1 MPa, the line graph of the proportion of oil with large particle size gradually rises before reaching 40 μm, after which the proportion decreases more rapidly. Despite the stratification of rolling elements, the rotation induces air resistance and centrifugal force, leading to a gradual decrease in the size of larger oil particles. This reduction exacerbates atomization within the cavity. At injection pressures of 0.3 MPa and 0.6 MPa, increasing the injection pressure increases the volume of oil entering the bearing cavity. Consequently, the volume of larger oil particles increases. Although the rolling elements are stratified, air resistance and the formation of eddy currents around them negatively impact the

lubrication of oil within the bearing cavity. The proportion of oil with larger particle size decreases slowly, and the increase in the amount of oil is beneficial to the lubrication of the bearing. Therefore, when the spray pressure is high, the atomization in the cavity is not intensified, which benefits the lubrication of the bearing.

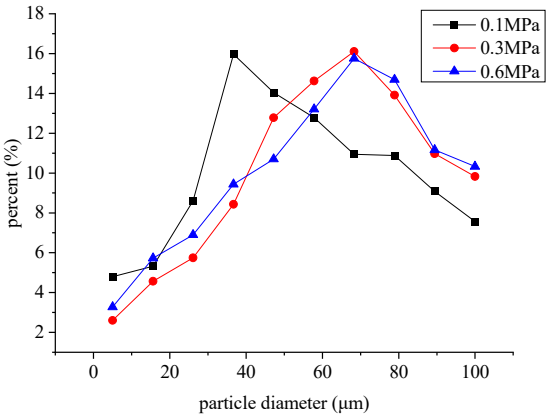

Figure 8. Variation of oil particle size in the bearing cavity under different injection pressures (6 layers of rolling elements).

Figure 9 shows the change in oil particle size in the bearing cavity when the rolling elements are divided into 10 layers. From the figure, it can be observed that under high injection pressure conditions, the oil injected into the bearing cavity initially increases due to the rise in injection pressure, resulting in an upward trend of the broken line. At an injection pressure of 0.1 MPa, particle sizes greater than 40 μm are influenced by the stratification of rolling elements, leading to airflow resistance that generates vortices near them. This phenomenon adversely affects lubrication within the bearing. Additionally, factors such as the cage effect and centrifugal force contribute to the breakdown and potential atomization of oil over time, resulting in a reduced proportion of larger oil particles and a more pronounced atomization effect in the bearing cavity. When the injection pressure is 0.3 MPa and 0.6 MPa, the oil intake only increases at the beginning, and the broken line also rises to a certain value, then the particle size of oil shows a downward trend. This is because the amount of oil in the bearing cavity is large, and the proportion of large particle size oil decreases more slowly. Therefore, an increase in oil injection pressure is beneficial to the lubrication of the bearing cavity.

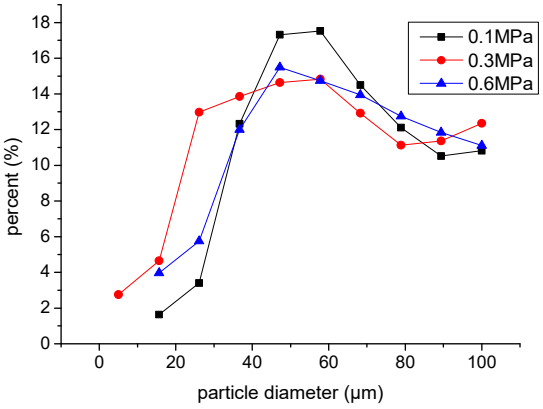

Figure 9. Variation of oil particle size in the bearing cavity under different injection pressures (the rolling elements are divided into 10 layers).

According to the comparative analysis of Figures 8 and 9, when the rolling body is stratified into six layers, the volume of larger oil particles exhibits a significant decrease over

time with changes in pressure. In contrast, when the rolling body is divided into 10 layers, the variation in the volume of larger oil particles occurs more gradually in response to pressure changes. With the change of pressure, the rolling elements are differently layered, and the particle size of the oil also changes, so the oil atomization in the cavity is not all the same.

5. Test Verification

5.1. Test Sample Selection

The LYC7306C angular contact ball bearing was used as the test bearing. The specific parameters of the test bearing are shown in Table 4. The bearing lubricant can be turbine oil.

Table 4. Test bearing parameters.

Parameter	Value
Bearing inner diameter d/mm	30
Bearing outer diameter D/mm	72
Bearing width B/mm	19
Contact angle α/°	15
Groove width/mm	0.65
Groove depth/mm	0.25
Dynamic bearing load rating Cr/kN	32.5
Bearing static load C_0/kN	20.3

A camera from the ACS-1 series of high-speed cameras produced by Japan's NAC company was used as shown in Figure 10 to monitor the changes in the size of the oil droplets in the bearing cavity. The software Cine Viewer Application (Ansys 19.2) was used, matched with the camera for processing, as shown in Figure 11.

Figure 10. ACS-1 high-speed camera.

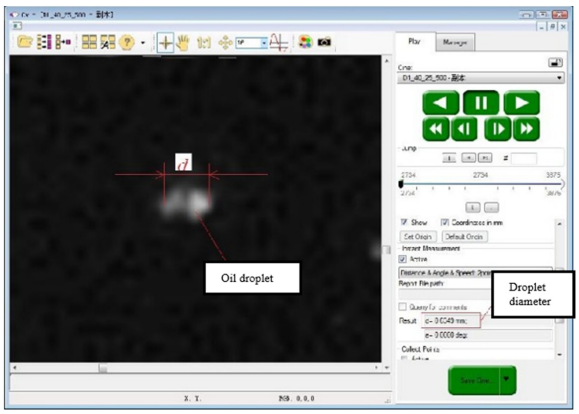

Figure 11. Cine Viewer Application software interface.

5.2. Test Conditions and Methods

This experiment was conducted using the BGT-1A bearing comprehensive performance testing machine. The spindle features frequency conversion speed regulation, and the test time can be preset, the load is stable, and the computer can automatically record and save the data. Figure 12 illustrates the improved device of the testing machine.

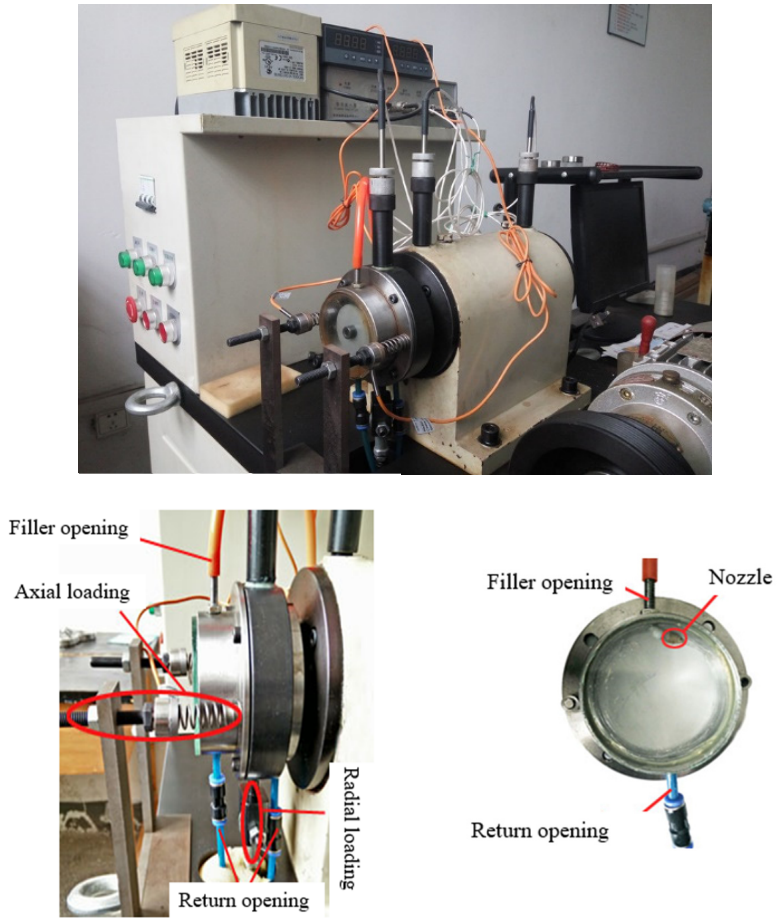

Figure 12. The modified loading and lubrication device.

The test primarily verifies the influence of bearing speed and injection pressure on the oil film thickness between the bearing rings, and it compares and analyzes the simulation results to validate their accuracy. Since the bearing operates at a high speed, it generates more severe vibrations in the test system; therefore, a specific initial load must be applied to ensure smooth operation of the bearing. To ensure the smooth operation of the bearing, extensive repeated measurements determined that the optimal axial load and radial load are 50 N and 100 N, respectively. The nozzle design is adjustable in the vertical direction to modify the spray angle.

The test bearing was operated for 12 h at a speed of 1000 r/min with an oil supply rate of 0.07 L/min. Relevant test conditions, including bearing speed and fuel injection pressure, were adjusted accordingly. A high-speed camera was activated through the tempered glass of the bearing end cap to capture the trend of oil entering the bearing chamber via the nozzle. Video processing software (CV 3.6.800) compatible with the high-speed camera was used to analyze the recorded oil flow. Figure 13 illustrates the principle of oil injection lubrication.

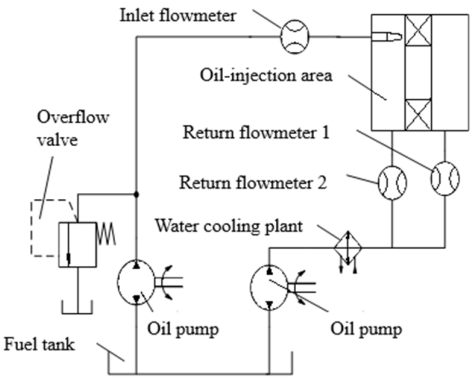

Figure 13. Principle diagram of oil injection lubrication.

5.3. Test Results and Analysis

Figure 14 illustrates the variation of the oil particle size ratio in the bearing cavity at a specific oil supply speed and varying rotational speeds; this change in the particle size ratio can be used to assess the oil atomization within the cavity. Through comparative simulation and testing, it was observed that as bearing speed increases, the ratio of larger particles in the bearing cavity gradually decreases while the proportion of smaller particles increases. Over time, particle fragmentation occurs, resulting in an intensified oil mist within the cavity. When the bearing speed is constant, the particle size ratio of larger oil particles in the simulation data is slightly greater than that in the experimental data, indicating that the oil particle size in the bearing cavity varies with speed. Furthermore, the data obtained from the experiment is smaller than that derived from the simulations. This discrepancy occurs because some oil ejected from the bearing chamber is captured by Flowmeter 2 on the return pipe, leading to a reduced actual oil volume within the bearing chamber. However, the trends of the simulation and experimental data are generally consistent, and the error is relatively small, thus validating the effectiveness of the simulation.

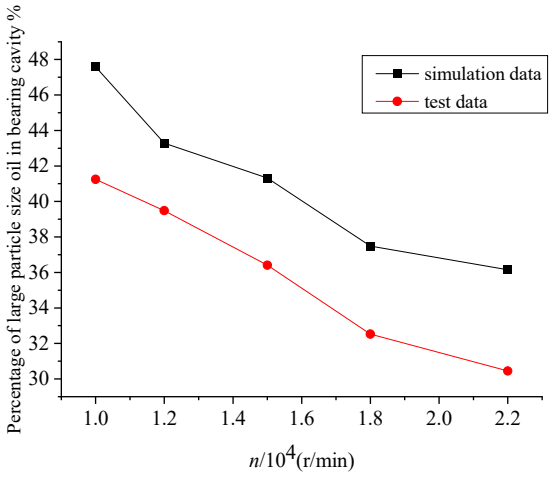

Figure 14. Variation of the proportion of oil with large particle size in the bearing cavity with speed.

Figure 15 shows the size change of large-particle oil in the bearing cavity under test conditions when the bearing speed is 2.2×10^4 r/min. It can be seen from the figure that under the same injection pressure, the proportion of large-particle oil in the bearing cavity obtained from the simulated data is slightly higher than that from the experimental data. With the increase in injection pressure, the proportion of large-particle oil in the rolling bearing chamber increases non-linearly; however, with the continuous increase in injection pressure, the proportion of large-particle oil in the bearing chamber increases slightly.

However, the value of the simulated data is slightly higher than that of the experimental data. The reasons are the same as above, so it will not be described too much.

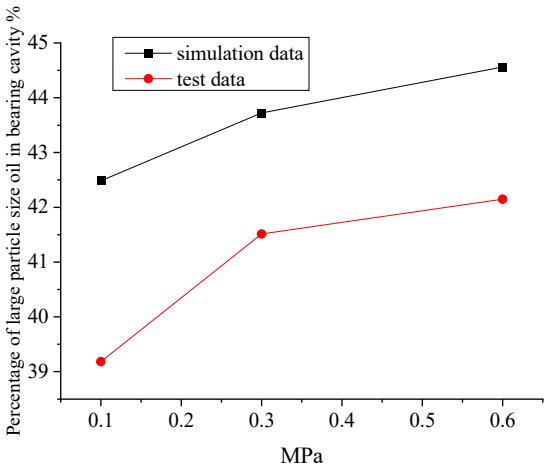

Figure 15. The proportion of large-particle oil in the bearing cavity varies with the injection pressure.

6. Conclusions and Prospects

The research in this paper is based on the previous numerical simulation method of gas–liquid two-phase flow between bearing rings, with further calculations and analysis of oil atomization in the bearing cavity in the case of rolling element stratification.

1. After the oil enters the bearing cavity and the rolling elements are stratified, the oil distribution in the cavity is relatively dispersed. Because of the different stratification of the rolling elements, the effect on the oil distribution in the cavity is different. Therefore, it is more intuitive to see the distribution of oil atomization in the bearing cavity, and it is beneficial to the research of bearing lubrication.
2. At different speeds and under varying stratification conditions, the number of rolling elements in the cavity increase over time, while the amount of larger oil particles decreases. The SMD (Sauter Mean Diameter) of the oil particle size decreases, and the improved atomization quality is not conducive to the lubrication. However, when the rolling elements are divided into 10 layers, their increased stratification leads to smaller vortices forming around them, resulting in a minimal impact on the oil entering the cavity; thus, the effect on bearing lubrication is relatively minor.
3. When the bearing is divided into 6 layers and 10 layers at different speeds, the distribution of large oil particles is not pronounced. As the rotational speed increases, the amount of oil entering the bearing cavity from the nozzle decreases, leading to a gradual reduction of large oil particles in the cavity. Additionally, due to the vortices created by stratification and the rotation of the rolling elements, the larger oil particles in the cavity are broken down, resulting in a more pronounced atomization distribution within the cavity. This phenomenon is detrimental to the lubrication of the bearing.
4. Under the same time and speed but with varying injection pressures, the rolling elements may be stratified differently; however, as the injection pressure increases, the amount of oil in the bearing cavity also increases, leading to a higher proportion of larger oil particles. Consequently, different injection pressures result in variations in the size of oil particles within the cavity. An increase in injection pressure is beneficial for the lubrication of the bearing.

This study opens several avenues for future research to enhance the understanding of oil atomization and lubrication in rolling bearings:

1. Atomization Techniques: Investigating various atomization methods can optimize oil distribution in bearing cavities. Experimental setups should assess how these

techniques influence droplet size and distribution, contributing to improved lubrication efficiency.
2. Dynamic Analysis of Layered Elements: Conducting detailed dynamic analyses of multi-layered rolling elements will clarify their impact on oil distribution and lubrication performance under different operational conditions.
3. Operational Conditions: Expanding the scope of studies to include diverse speeds, loads, and temperatures will provide insights into how these factors affect oil atomization and lubrication, leading to better bearing design.
4. Injection Pressure Optimization: Research should focus on optimizing injection pressure settings tailored to specific applications, developing guidelines that enhance lubrication by adjusting pressure based on operational requirements.
5. Advanced Lubricants: Exploring advanced lubricants or additives could reveal ways to improve oil atomization and lubrication performance across varying conditions, with potential benefits for bearing efficiency and longevity.

By pursuing these directions, we can achieve a deeper understanding of the interplay between oil atomization and bearing lubrication, ultimately enhancing mechanical performance and reliability across various applications.

Author Contributions: Methodology, F.W.; Software, F.W. and Y.L.; Validation, F.W.; Data curation, F.W. and Y.L.; Writing—original draft, F.W.; Writing—review & editing, H.L.; Supervision, H.L. All authors have read and agreed to the published version of the manuscript.

Funding: This study was supported by a special program from the Ministry of Science and Technology of China (Approval No. 2017ZHZX04).

Data Availability Statement: The data used to support the findings of this study are included within the article.

Conflicts of Interest: The authors declare no conflicts of interest.

References

1. Pinel, S.I.; Signer, H.R.; Zaretsky, E.V. Comparison between oil-jet lubrication of high-speed, small-bore, angular-contact ball bearings. *Tribol. Trans.* **2001**, *44*, 327–338. [CrossRef]
2. Darul, L.; Touret, T.; Changenet, C.; Ville, F. Power Loss Analysis of an Oil-Jet Lubricated Angular Contact Ball Bearing: Theoretical and Experimental Investigations. *Lubricants* **2024**, *12*, 14. [CrossRef]
3. Glahn, A.; Witting, S. Two-phase air/oil flow in aero engine bearing chambers: Characterization of oil film flows. *Trans. ASME J. Eng. Gas Turbines Power* **1996**, *118*, 578–583. [CrossRef]
4. Gong, B.B.; Zhang, J.G.; Wang, J.W. Research and development of an experimental device for a rolling bearing lubricated with oil and air. *Mech. Sci. Technol.* **2007**, *26*, 181–183.
5. Jianwen, W.; Qi, A. Investigation of two-phase flow regimes in transport pipe in oil-air lubrication system. *J. East China Univ. Sci. Technol. Nat. Sci. Ed.* **2009**, *35*, 324–327.
6. Xie, J.; Jiang, S.; Wang, X.; Feng, Y. Experimental research on oil-air lubrication for high-speed ball bearing. *Lubr. Eng.* **2006**, *181*, 114–119.
7. Wang, Y.; Niu, W.; Tang, W.; Guo, M.; Guo, X.; Li, G.; Shen, R. Research on oil-air multiphase flow of spray lubrication of aero spur gears. *J. Aerosp. Power* **2013**, *28*, 439–444.
8. Wu, H.; Chen, G. Homogeneous flow of two-phase gas/liquid flow in aero-engine bearing chamber. *J. Tribol.* **2007**, *27*, 78–82.
9. Glahn, A.; Kurreck, M.; Willmann, M.; Wittig, S. Feasibility study on oil droplet flow investigations inside aero engine bearing chambers–PDPA techniques in combination with numerical approaches. *J. Eng. Gas Turbines Power* **1996**, *118*, 749–755. [CrossRef]
10. Glahn, A.; Busam, S.; Blair, M.F.; Allard, K.L.; Wittig, S. Droplet Generation by Disintegration of Oil Films at the Rim of a Rotating Disk. *J. Eng. Gas Turbines Power* **2002**, *124*, 117–124. [CrossRef]
11. Glahn, A.; Blair, M.F.; Allard, K.L.; Busam, S.; Schafer, O.; Wittig, S. Disintegration of Oil Jets Emerging from Axial Passages at the Face of a Rotaing Cylinder. *J. Eng. Gas Turbines Power* **2003**, *125*, 1003–1110. [CrossRef]
12. Glahn, A.; Blair, M.F.; Allard, K.L.; Busam, S.; Schafer, O.; Wittig, S. Disintegration of Oil Films Radial Holes in a Rotating Cvlinder. *J. Eng. Gas Turbines Power* **2003**, *125*, 1011–1120. [CrossRef]
13. Szydlo, Z.A. Effective oil/air ratio in industrial oil mist lubricating systems. *Ind. Lubr. Tribol.* **2007**, *59*, 4–11. [CrossRef]
14. Lee, J.; Kaug, S.; Rho, B. Atomization characteristics of intermittent multi-hole diesel spray using time-resolved PDPA data. *J. Mech. Sci. Technol.* **2003**, *17*, 766–775. [CrossRef]
15. Di, D.; Liu, Y.; Wang, Y. Experiment on atomization characteristics of fan nozzle. *J. Aerosp. Power* **2020**, *3*, 457–470.
16. Chen, L.; Yang, C.; Long, W. Experiment on atomization of high disturbance fuel nozzle. *J. Aerosp. Power* **2019**, *34*, 2091–2097.

17. Liu, H.B.; Liu, G.P.; Li, Y.B.; Wang, L. Numerical simulation of two-phase air/oil flow in high speed angular contact ball bearing chamber. *J. Aerosp. Power* **2018**, *33*, 1103–1111.
18. Liu, H.B.; Liu, G.P.; Hao, J.H.; Yang, M.K. Oil penetration mechanism induced by different bearing wall grooves. *J. Aerosp. Power* **2019**, *34*, 1127–1136.
19. Victor, Y.; Steven, A.O. Renormalization group analysis of turbulence: Basic theory. *J. Sci. Comput.* **1986**, *1*, 3–11.
20. Liu, H.; Zhang, L.; Shi, Y.; Wang, H. Numerical simulation of airflow characteristics between rings of the high-speed rolling bearing. *J. Mech. Des.* **2016**, *33*, 61–66.